

# Low frequency acoustic energy harvesting using PZT piezoelectric plates in a straight tube resonator

Bin Li<sup>1</sup>, Jeong Ho You<sup>1</sup> and Yong-Joe Kim<sup>2</sup>

<sup>1</sup> Department of Mechanical Engineering, Southern Methodist University, Dallas, TX 75205, USA

<sup>2</sup> Department of Mechanical Engineering, Texas A&M University, College Station, TX 77843, USA

E-mail: [jyou@smu.edu](mailto:jyou@smu.edu)

Received 2 November 2012, in final form 2 March 2013

Published 5 April 2013

Online at [stacks.iop.org/SMS/22/055013](http://stacks.iop.org/SMS/22/055013)

## Abstract

A novel and practical acoustic energy harvesting mechanism to harvest traveling sound at low audible frequency is introduced and studied both experimentally and numerically. The acoustic energy harvester in this study contains a quarter-wavelength straight tube resonator with lead zirconate titanate (PZT) piezoelectric cantilever plates placed inside the tube. When the tube resonator is excited by an incident sound at its acoustic resonance frequency, the amplified acoustic pressure inside the tube drives the vibration motions of piezoelectric plates, resulting in the generation of electricity. To increase the total voltage and power, multiple PZT plates were placed inside the tube. The number of PZT plates to maximize the voltage and power is limited due to the interruption of air particle motion by the plates. It has been found to be more beneficial to place the piezoelectric plates in the first half of the tube rather than along the entire tube. With an incident sound pressure level of 100 dB, an output voltage of 5.089 V was measured. The output voltage increases linearly with the incident sound pressure. With an incident sound pressure of 110 dB, an output voltage of 15.689 V and a power of 12.697 mW were obtained. The corresponding areal and volume power densities are  $0.635 \text{ mW cm}^{-2}$  and  $15.115 \mu\text{W cm}^{-3}$ , respectively.

(Some figures may appear in colour only in the online journal)

## 1. Introduction

There have been tremendous efforts in harvesting environmental energies including radiant (e.g. solar [1]), mechanical (e.g. wind [2] and vibration [3]), thermal [4] and biochemical energies [5]. However, our environment is still full of wasted and unused energy. One of the environmental energy sources which has been less investigated compared with other resources, is acoustic energy. As a clean, ubiquitous and renewable energy, acoustic energy is prevalent in our life and currently wasted. In recent years, increasing efforts have been expended on developing mechanisms to harvest the acoustic energy available in airports, construction sites, factory, traffic etc. Horowitz *et al* [6] first introduced a micromachined acoustic energy harvester using a Helmholtz

resonator with a lead zirconate titanate (PZT) piezoelectric composite diaphragm attached to the resonator's bottom wall. An output power of  $\sim 0.1 \text{ nW}$  was obtained with an incident sound pressure level (SPL) of 149 dB (referenced  $20 \mu\text{Pa}$  [7]) at 13.6 kHz. The corresponding power density was  $0.34 \mu\text{W cm}^{-2}$ . An electromechanical Helmholtz resonator (EMHR) has been developed to utilize the resonant cavity pressure to deform a PZT piezoelectric back plate [8–10]. With an external sound with a 160 dB SPL at 2.6 kHz, the EMHR generated a power of 30 mW. Kim *et al* [11] also used a Helmholtz resonator and an electromagnetic generator to harvest airflow and aeroacoustic energy. In their harvester, the vibration motion of the resonator cavity wall drives the permanent magnet/coil generator and an output voltage of 4 mV was measured with a 140 dB SPL at 1.4 kHz.

In addition to a Helmholtz resonator, a sonic crystal has been used to convert acoustic energy to electricity [12–14]. A curved polyvinylidene fluoride (PVDF) piezoelectric beam was placed inside a defect region of a sonic crystal, which acts as a resonant cavity. The sound pressure inside the defect region was amplified by 4.94 times and excited the PVDF beam at structural resonance. An output power of  $\sim 35$  nW was obtained with an incident SPL of 80–100 dB at 4.2 kHz. A nonlinear treatment for electric circuit design was used to optimize the acoustic energy harvesting efficiency. Lallart *et al* [15] used synchronized switch harvesting on an inductor (SSHI) with the PZT-membrane acoustic energy harvester and increased the power gain up to 10 and the bandwidth by 100%. An output power of  $\sim 60$   $\mu$ W with an areal power density of  $0.7$   $\mu$ W cm $^{-2}$  have been obtained with an incident SPL of 100 dB at 240 Hz. Most previous systems harvest acoustic energy at high frequencies (few kHz) and/or their harvesting power densities are low. Therefore, it is necessary to investigate a highly efficient acoustic energy harvesting mechanism which can convert a low audible frequency sound to electricity.

In this study, a straight tube acoustic resonator with PZT piezoelectric cantilever plates has been used to harvest acoustic energy from a low frequency traveling sound. The straight tube is 42 cm long with one end open and the other end closed, and its first acoustic resonance frequency is 199 Hz. The harvesting frequency can be easily tuned by changing the tube length. When the tube is excited by an external sound wave at its eigenfrequency, a resonant standing wave is developed inside the tube. When PZT cantilever plates are placed perpendicular to the tube axis, the resonant standing wave excites the vibration motion of the PZT plates, resulting in the generation of electricity.

This paper is organized as follows. The theoretical background including the acoustic resonant behavior of a straight tube resonator and the energy conversion of piezoelectric cantilever plates are described in section 2. The experimental apparatus and procedures are discussed in section 3. Numerical simulations using the finite element method are discussed in section 4. Experimental and numerical results are compared and discussed in section 5. The conclusions are drawn in section 6.

## 2. Theoretical background

### 2.1. Quarter-wavelength straight tube resonator

Acoustic resonators have been widely used for both sound augmentation in musical instruments [16] and noise attenuation in industrial applications [17]. When an acoustic resonator is excited by an incident wave at its acoustic resonant frequencies, acoustic energy is collected inside the resonator in the form of resonant standing waves. For a straight tube with one end open and the other closed as shown in figure 1(a), the acoustic pressure  $p_n(z)$  and the longitudinal particle velocity  $u_n(z)$  at the  $n$ th resonant mode

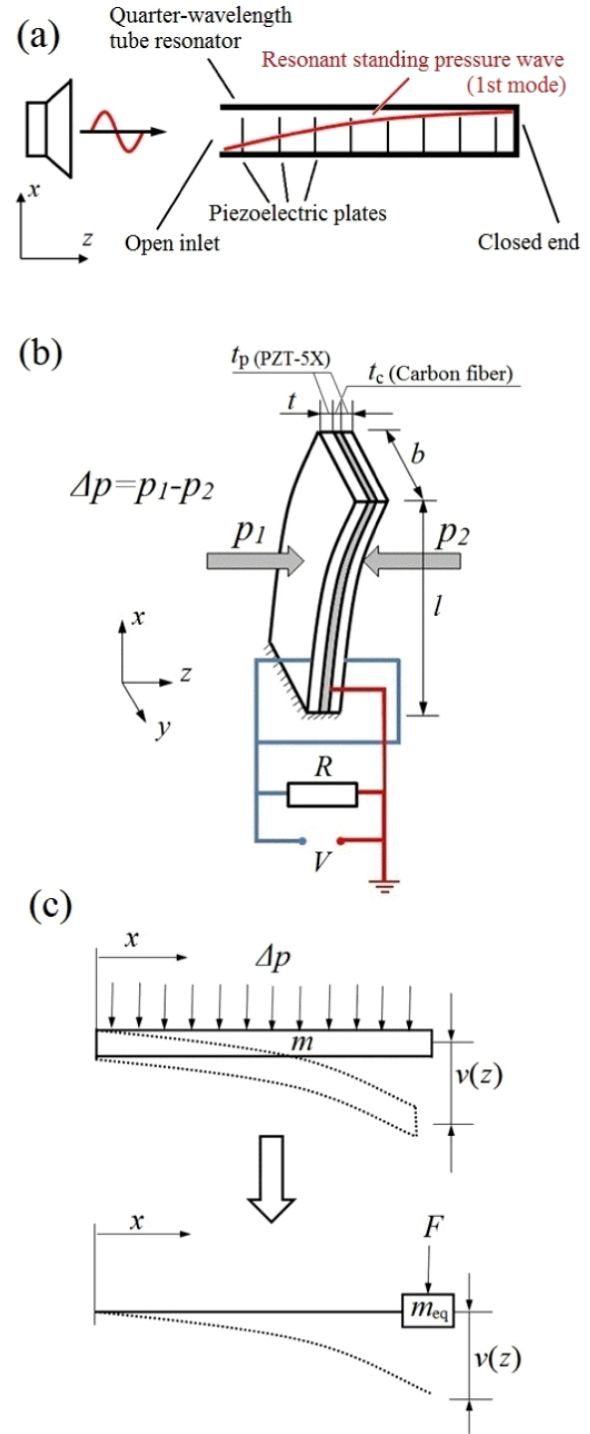


**Figure 1.** (a) Schematic drawing of a quarter-wavelength straight tube resonator with piezoelectric plates placed inside the tube vibrated by the resonant standing pressure wave (first mode), (b) structure and circuit connection of a parallel bimorph PZT piezoelectric cantilever plate deformed by acoustic pressure difference  $\Delta p$  and (c) sketch for the equivalent transform of cantilever plate from distributed mass to point mass.

are represented as sinusoidal functions as [18, 19]

$$p_n(z) = p_{0n} \sin \frac{\pi(2n-1)z}{2L}, \quad (1)$$

$$u_n(z) = u_{0n} \cos \frac{\pi (2n-1)z}{2L}, \quad (2)$$

with the corresponding resonance frequency  $f_n$  being expressed as

$$f_n = \frac{(2n-1)c_0}{4L}, \quad (3)$$

where  $z$  is the distance measured from the open inlet along the tube,  $L$  is the tube length which is equal to  $(2n-1)\lambda/4$ ,  $c_0$  is the speed of sound and  $n$  is the integer mode number  $n = 1, 2, 3, \dots$ . At the first eigenmode (i.e.  $n = 1$ ), the tube length is equal to the quarter wavelength  $L = \lambda/4$ , so it is called a quarter-wavelength resonator. In equations (1) and (2), the pressure release boundary condition (i.e.  $p_n = 0$ ) is assumed at the open inlet ( $z = 0$ ) and the rigid boundary condition (i.e.  $u_n = 0$ ) at the closed end ( $z = L$ ). From equations (1) and (2), the maximum acoustic pressure occurs at the closed end while the particle velocity becomes the maximum at the open inlet.

## 2.2. Energy conversion by cantilever piezoelectric plates

In order to harvest acoustic energy in the tube, piezoelectric cantilever plates are placed along the straight tube resonator as shown in figure 1(a). When a piezoelectric cantilever plate is placed inside the tube resonator, the spatially varying acoustic pressure in equation (1) generates the pressure difference  $\Delta p$  between each side of the plate and drives the vibrational motion of the piezoelectric plate, resulting in electricity generation by the 31 piezoelectric mode. To maximize the harvested energy, each piezoelectric plate is designed to have the same structural resonance frequency as the acoustic resonance frequency of the tube. When the piezoelectric plate is placed near the tube inlet where the pressure gradient is at a maximum, a large displacement of plate will generate a high voltage.

The output power from piezoelectric generators significantly depends on the electrical impedance of the external loading circuit [10, 13, 20–23]. To find the optimal external loading, the output power from the piezoelectric cantilever plates inside the tube should be expressed as a function of pressure difference  $\Delta p$ . The equivalent circuit model for mechanical and electrical elements of a piezoelectric cantilever plate can be described as [20, 21]

$$\sigma_{in} = \sigma_i + \sigma_d + \sigma_s + \sigma_p, \quad (4)$$

where  $\sigma_{in}$  is an input stress and  $\sigma_i$ ,  $\sigma_d$ ,  $\sigma_s$  and  $\sigma_p$  are the equivalent stresses to inertial, damping, stiffness and piezoelectric elements, respectively. The input stress  $\sigma_{in}$  can be regarded as the average normal stress induced by bending moment  $M_p(x)$  as

$$\sigma_{in} = \frac{1}{I} \int_0^l \frac{M_p(x)t_m}{I} dx, \quad (5)$$

where  $I$  is the moment of inertia of the whole piezoelectric plate as  $I = 2(bt_p^3/12 + bt_p t_m^2) + \alpha bt_c^3/12$ ,  $b$  is the width of the piezoelectric plate,  $t_p$  and  $t_c$  are the thicknesses of

the piezoelectric layer and carbon fiber,  $\alpha$  is the ratio of the Young's moduli of the piezoelectric layer and carbon fiber,  $t_m$  is the distance from the neutral axis to the center of the piezoelectric layer,  $l$  is the total length of the piezoelectric plate.  $M_p(x)$  is the equivalent bending moment induced by the acoustic pressure difference  $\Delta p$ .

In order to obtain  $\sigma_i$ ,  $\sigma_d$ ,  $\sigma_s$  and  $\sigma_p$ , the cantilever plate with distributed mass under uniform acoustic pressure is simplified to the plate with an equivalent point mass  $m_{eq}$  under a concentrated force  $F$ , as shown in figure 1(c). The equivalent point mass can be obtained by equating kinetic energy from both systems. The displacement  $v(\tau, x)$  for the cantilever plate under  $\Delta p$  is [24]

$$v(\tau, x) = \frac{bx^2(6l^2 + 4lx + x^2)}{24EI} \Delta p, \quad (6)$$

where  $E$  is the Young's modulus of the whole piezoelectric plate and  $b$  is the plate width. Kinetic energy  $G_k$  can be obtained by integrating the kinetic energy of an element  $dx$  as

$$G_k = \int_0^l dG_k = \int_0^l \frac{\dot{v}(\tau, x)^2}{2} \frac{m dx}{l} = \frac{\dot{v}(\tau, l)^2}{2} 0.257 m, \quad (7)$$

where  $m$  is the total mass of the piezoelectric plate. Therefore, the equivalent point mass is  $m_{eq} = 0.257 m$ . The induced stresses in equation (4) are given as

$$\begin{aligned} \sigma_i &= \frac{m_{eq}}{c_1} \ddot{\delta}, & \sigma_d &= \frac{\beta}{c_2} \dot{\delta}, & \sigma_s &= E_p \delta, \\ \sigma_p &= \frac{-d_{31} E_p}{t_p} V \end{aligned} \quad (8)$$

where  $\delta$  is strain,  $t_p$  is the thickness of the piezoelectric material,  $d_{31}$  is the piezoelectric constant,  $E_p$  is Young's modulus of the piezoelectric layer, the damping coefficient is  $\beta = 2\zeta \omega_n m_{eq} c_2 / c_1$  with the damping ratio  $\zeta$  and the geometric constants  $c_1 = 3I/l^3$  and  $c_2 = 3t_c/(2l^2)$ . Substituting equations (5) and (8) into equation (4) gives the magnitude of the output voltage as a function of the acoustic pressure difference  $\Delta p$  as

$$\begin{aligned} V_{mag} &= \frac{\omega_n R C_p d_{31} t_p / \varepsilon}{\sqrt{R^2 C_p^2 \omega_n^2 (4\zeta^2 + k^2) + 4\zeta^2 + 4\zeta k^2 \omega_n R C_p}} \\ &\times \left( \frac{t_c l^2 b}{6I} \right) \Delta p, \end{aligned} \quad (9)$$

where  $k$  is the piezoelectric coupling coefficient,  $C_p$  is the piezoelectric capacitance,  $R$  is the loading resistance and  $\varepsilon$  is the permittivity. Then, the output electric power  $P$  is given as

$$\begin{aligned} P &= \frac{V_{mag}^2}{R} = \frac{(\omega_n d t_p / \varepsilon)^2 R C_p^2}{\omega_n^2 R^2 C_p^2 (4\zeta^2 + k^4) + 4\zeta^2 + 4k^2 \zeta \omega_n R C_p} \\ &\times \left( \frac{t_c l^2 b}{6I} \Delta p \right)^2. \end{aligned} \quad (10)$$

The maximum amount of power can be obtained when  $\partial P / \partial R = 0$  with the optimized resistance as

$$R_{opt} = \frac{1}{\omega_n C_p} \frac{2\zeta}{\sqrt{4\zeta^2 + k^4}}. \quad (11)$$

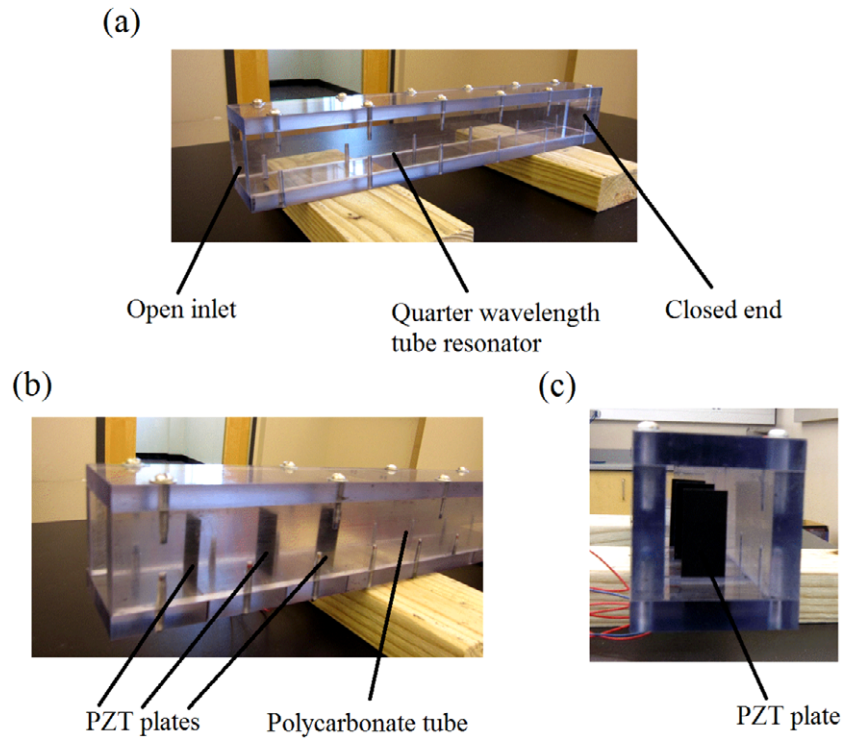


**Figure 2.** (a) A quarter-wavelength straight tube resonator with one end open and the other end closed. (b) Perspective and (c) front views of the straight tube resonator with PZT piezoelectric plates installed.

**Table 1.** Dimension and material properties of the parallel bimorph PZT piezoelectric plate and polycarbonate panel.

Parallel bimorph piezoelectric plate					
Length	$l$	4 cm	Piezoelectric constant	$d_{31}$	$-320 \text{ pC N}^{-1}$
Width	$b$	2 cm	Coupling coefficient	$k$	0.321
Thickness	$t$	0.7 mm	Permittivity	$\varepsilon/\varepsilon_0$	4500
Damping ratio	$\zeta$	0.025			
PZT-5X layer					
Thickness	$t_p$	0.48 mm	Density	$\rho_p$	$7400 \text{ kg m}^{-3}$
Young's modulus	$E_p$	40 GPa	Capacitance	$C_p$	75 nF
Carbon fiber					
Thickness	$t_c$	0.22 mm	Young's modulus	$E_c$	2 GPa
Polycarbonate					
Density	$\rho_{pc}$	$1175 \text{ kg m}^{-3}$	Young's modulus	$E_{pc}$	2.2 GPa

### 3. Experiments

A quarter-wavelength straight tube resonator has been fabricated using 1/2 in thick polycarbonate panels. The tube is 42 cm long with a rectangular cross-section of 4 cm  $\times$  5 cm, as shown in figure 2(a). Thick acoustical sealing caulk is applied between the gaps of the polycarbonate panels to minimize sound leakage. A loudspeaker (JBL JRX118S 18 in Compact Subwoofer driven by a Crown XLS 1000 DriveCore Series power amplifier by *Harman*) is used to generate an incident sound wave. Quarter-inch condenser microphones (377C10 by *PCB Piezotronics*) powered by a sensor signal conditioner

(482C05 by *PCB Piezotronics*) are used to measure acoustic pressures at various positions along the tube.

In order to convert the acoustic energy inside the tube resonator, parallel bimorph PZT piezoelectric cantilever plates (Stripe Actuator 40-2010 by *APC International Ltd*) have been installed perpendicular to the tube axis as shown in figures 2(b) and (c). The PZT plate consists of the carbon fiber central shim sandwiched between two PZT-5X piezoelectric layers as shown in figure 1(b). Two electrodes are connected to both sides of the plate and the central shim is connected to ground. The dimensions and material properties of the PZT piezoelectric plates and polycarbonate panel are provided in table 1. To clamp the PZT piezoelectric plates, the bottom



panel of the tube consists of several polycarbonate blocks with small notches. The PZT plates were inserted in the notches and clamped by the bottom blocks. A data acquisition system (NI-PCI 6289) is used to measure the output voltage from the PZT plates.

#### 4. Numerical simulations

Numerical simulations have been performed by finite element analysis using COMSOL *multiphysics* 4.3. In order to simulate the energy harvesting from traveling sound waves, the straight tube resonator is surrounded by a large cylindrical domain where the by-passing sound and the diffracted sound by the tube inlet can travel and leave the domain. The outer boundary of the cylindrical domain is set as a radiation boundary to minimize the reflection back into the domain. Since the air motion near the tube inlet also generates sound radiation in the radial direction outward from the inlet [19], a semi-spherical domain is attached to the cylindrical domain and a perfect matched layer (PML) is used to absorb the radial sound radiation from the tube inlet. An incident plane wave is generated in the semi-spherical domain and travels to the tube's open inlet at normal incidence as shown in figure 3(a). The PZT cantilever plates are placed along the tube axis as shown in figures 3(b) and (c). The tube wall material (1/2 in thick polycarbonate) is also included in simulations to consider any sound leakage/transmission through the tube walls.

#### 5. Results and discussions

##### 5.1. Acoustic resonance in a straight tube resonator

The first three resonant frequencies  $f_n$  ( $n = 1, 2$  and  $3$ ) and the corresponding pressure modes in the  $4\text{ cm} \times 5\text{ cm} \times 42\text{ cm}$  rectangular straight tube are shown in figure 4(b). The incident SPL is 100 dB. From both experiments and simulations, the acoustic resonant pressure distributions along the tube follow the sinusoidal functions in equation (1) with the maximum at the closed tube end. The amplification ratio which is the ratio of the maximum pressure in the tube to the incident sound pressure ( $A = p_{\text{max}}/p_{\text{incident}}$ ), is experimentally measured as 97.2, 51.0 and 11.2 at  $f_1 = 199\text{ Hz}$ ,  $f_2 = 593\text{ Hz}$  and  $f_3 = 989\text{ Hz}$ , respectively. The calculated amplification ratios are 100.1, 56.2 and 13.0 at  $f_1 = 198\text{ Hz}$ ,  $f_2 = 593\text{ Hz}$  and  $f_3 = 981\text{ Hz}$  which match well with the experimental data. The highest amplification ratio in the first mode indicates that the most acoustic energy is accumulated inside the tube when the tube is excited at the first mode. Therefore, the first eigenmode is chosen as the harvesting mode in this study. Since the driving force for a piezoelectric plate is the pressure difference, a large driving force will be available near the open inlet where the pressure gradient is at a maximum as shown in figure 4(c). Near the closed end, the driving force is negligible although the pressure itself is at a maximum.

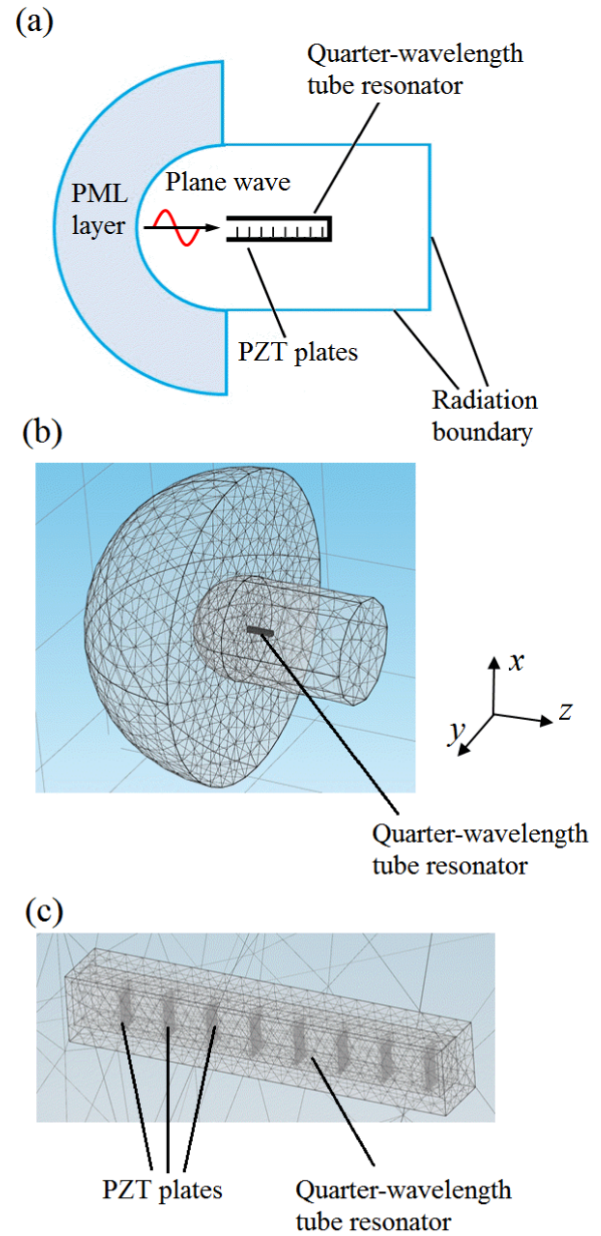


**Figure 3.** (a) Schematic of numerical simulations with boundary conditions, (b) a finite element mesh used in simulations and (c) a zoom-in view of a straight tube with eight piezoelectric plates.

##### 5.2. Energy harvesting using a single PZT piezoelectric plate

A single PZT piezoelectric plate has been placed at various positions inside the straight tube resonator to harvest the incident sound with 100 dB SPL at the first resonant frequency of the tube. The piezoelectric plate was first placed at 5 cm from the open inlet and moved toward the closed end with a moving distance of 5 cm. Placing a piezoelectric plate inside the tube changes the resonance behavior of the tube due to the disturbance of air particle motion. To ensure that the tube was excited resonantly, the incident frequency was increased from 180 to 205 Hz by 1 Hz in both experiments and calculations to confirm that the maximum voltage was obtained. From the measured voltage, the output power was obtained by  $V^2/R_{\text{opt}}$

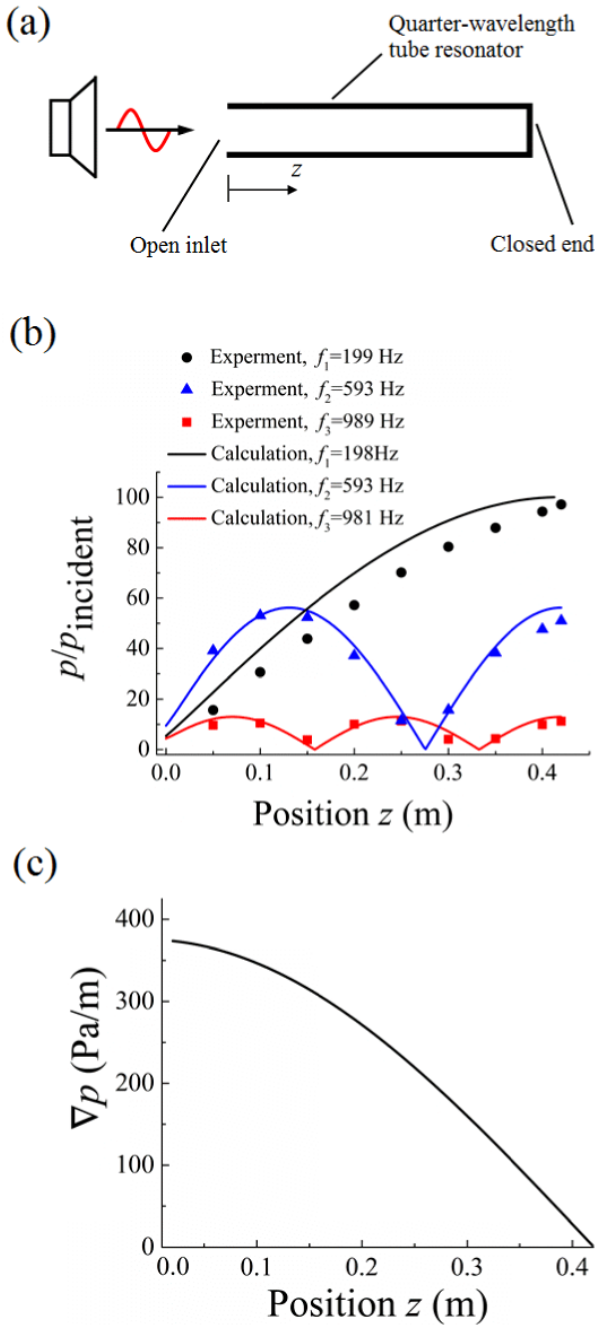


**Figure 4.** (a) Schematic of a straight tube resonator excited by a loudspeaker, (b) experimental and calculated pressure magnitudes normalized by the incident sound pressure at the first three eigenmodes along the tube and (c) calculated pressure gradient at the first mode. The tube is 42 cm long with a rectangular cross-section of 4 cm  $\times$  5 cm. The incident SPL is 100 dB.

with an optimized resistance of  $R_{\text{opt}} = 4.6 \text{ k}\Omega$  at  $f = 199 \text{ Hz}$  from equation (11).

The comparison between experimental data and calculated results is shown in figure 5(b) with a single piezoelectric plate placed at various positions along the tube. When the piezoelectric plate is placed at  $z = 5 \text{ cm}$  from the tube inlet, the calculated voltage and power are 1.639 V and 0.577 mW at an incident frequency of 196 Hz, while 1.51 V and 0.498 mW are measured from experiments at 199 Hz. As

the piezoelectric plate moves toward the closed tube end, the output voltage and power decreases. The decrease in voltage follows the pressure gradient (figure 4(c)) which confirms that the driving force is from the pressure difference. When the PZT plate is placed near the tube inlet where the pressure gradient is at a maximum, the largest output voltage and power are obtained due to the largest pressure gradient. When the plate is placed near the tube's closed end, the small pressure gradient induces a small plate deflection, although the pressure magnitude itself is at a maximum at the closed tube end.

To investigate the effect of a quarter-wavelength tube resonator in energy harvesting efficiency, a single piezoelectric plate is placed in an open area and excited directly by a traveling wave of 100 dB. The measured voltage and power are 0.038 V and  $0.313 \mu\text{W}$  respectively, which are 40 times and 1600 times lower than those when it is placed inside the tube resonator.

### 5.3. Energy harvesting using multiple piezoelectric plates

Multiple piezoelectric plates have been placed inside the tube resonator to increase the total output voltage and power. The incidence SPL is 100 dB and the incidence frequency is varied from 180 to 205 Hz by 1 Hz to obtain the maximum total output voltage and power. At the most, eight piezoelectric plates have been placed inside the tube, as shown in figure 6(a). The first position A is at 5 cm from the open inlet and the other positions (from B to H) are placed at increments of 5 cm. Figure 6(b) shows the experimental and calculated voltages as a function of the number of piezoelectric plates installed in the tube. The piezoelectric plates have been installed by filling the positions closer to the open inlet. For example, the number of piezoelectric plates equal to 3 indicates that three plates are placed at the positions A, B and C.

It can be observed that there is a certain number of piezoelectric plates that generates the maximum total voltage. From the experiments, the total output voltage increased until six plates were installed at the positions A through F. The maximum voltage of 3.79 V was measured from the six plates at an incidence frequency of 193 Hz. From the numerical simulations, the maximum voltage of 4.06 V was obtained by placing five plates (from A through E) with an incidence frequency of 189 Hz. In both experiments and simulations, placing any additional plates reduces the total output voltage. This is due to the alteration of acoustic resonance induced by placing the additional plates near the closed end. Although it is desired to install more piezoelectric plates to harvest more acoustic energy available in the resonator, the presence of the plates reduces the acoustic resonant pressure by interrupting the air particle motion along the tube. This effect can also be seen from the comparison between the first and second bars of figure 6(b). Installing the additional plate at B has decreased the voltage generated by the plate at A. From the measured voltage, the total power has been obtained as the summation of power from each plate ( $\sum V_i^2 / R_{\text{opt}}$ ,  $i = 1, 2, 3, \dots$ ) as shown in figure 6(c). Both experimental and calculated powers

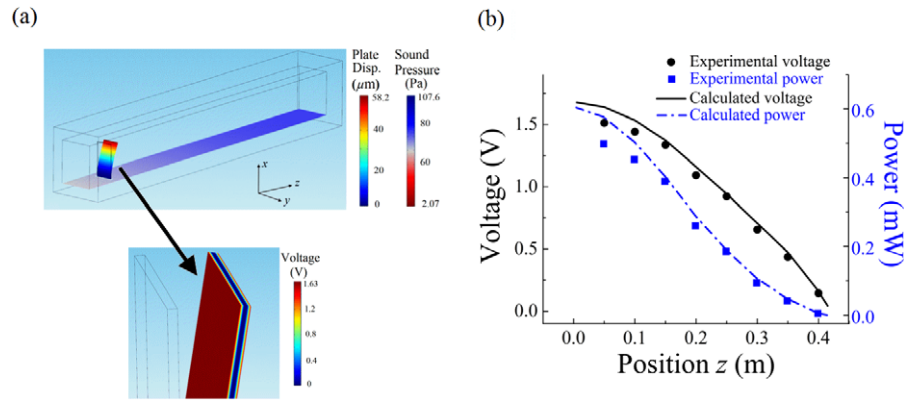


**Figure 5.** (a) An example of the calculated displacement and output voltage of one piezoelectric plate placed at 5 cm from the tube inlet and the corresponding sound pressure and (b) comparison between experimental and calculated voltage and power by a single piezoelectric plate at various positions along the tube. The incident SPL is 100 dB.

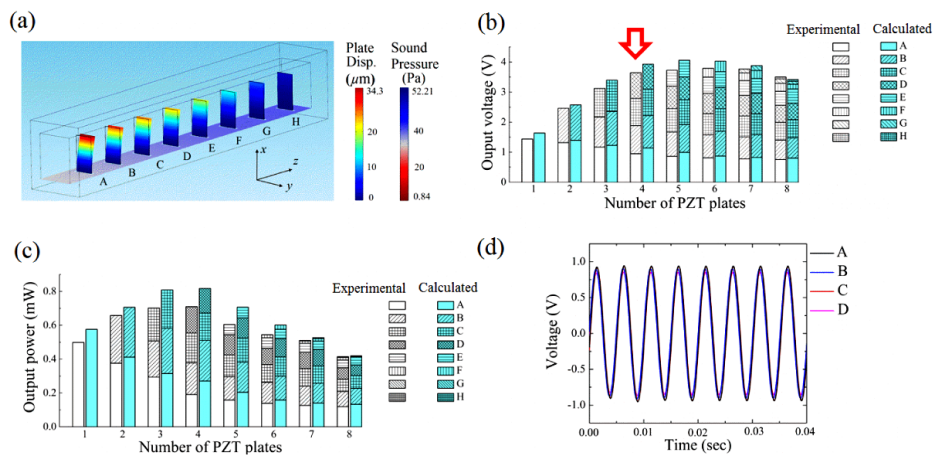


**Figure 6.** (a) An example of the calculated displacements of eight piezoelectric plates placed along the tube and the sound pressure. Experimental and calculated (b) voltage and (c) power with an incident SPL of 100 dB as a function of the number of piezoelectric plates installed inside the tube. (d) An example of the measured output voltage from four piezoelectric plates installed at positions A ( $z = 5$  cm) through D ( $z = 20$  cm), corresponding to the experimental results in (b) indicated by the red arrow.

become maximum as 0.710 mW and 0.819 mW respectively, when four plates are installed at the positions A through D. In terms of power, placing more piezoelectric plates also increases the resistance in the system. Therefore, placing the plates near the closed tube end where the output voltage is relatively low, reduces the total power due to the increased resistance.

Figure 6(d) shows the example of measured voltages from each piezoelectric plate when four piezoelectric plates are placed inside the tube at the positions A to D. It can be seen that the output voltages from individual piezoelectric plates are almost in the same phase, which indicates that all plates are vibrating in phase at their structural resonances.

Since placing additional piezoelectric plates near the closed tube end decreases the total power, the piezoelectric plates are placed only in the first half of the tube with the increased plate density as shown in figure 7(a). The first position A is located at 2.5 cm from the tube inlet and additional positions are set at increments of 2.5 cm in order to fill the first half of the tube. As shown in figures 7(b) and (c), the maximum total output voltage has

increased significantly to 5.089 V in experiments and 5.552 V in simulations, which are 34.3% and 36.7% increments, respectively. There are also significant improvements in power to 1.148 mW in experiments and 1.329 mW in simulations, which are 61.7% and 62.1% increments. Considering the cross-sectional area of tube inlet, the corresponding areal power density is  $0.0574 \text{ mW cm}^{-2}$  in experiments and  $0.0665 \text{ mW cm}^{-2}$  in simulations with an incident SPL of 100 dB. The volume power density is  $1.367 \mu\text{W cm}^{-3}$  in experiments and  $1.581 \mu\text{W cm}^{-3}$  in simulations. This volume power density at 100 dB SPL is at least one order of magnitude higher than the others [6, 8, 12, 13, 15], even at the lower operating frequency in this study. When the four piezoelectric plates are placed in an open area and directly excited by the traveling wave, a power of  $0.732 \mu\text{W}$  was measured which is 1570 times lower than that when they are placed in the tube resonator.

Figure 7(d) shows the experimental and calculated output voltage and power as a function of incident sound pressure using the four plates at the positions A ( $x = 2.5$  cm) through D ( $x = 10$  cm). The output voltage is linearly proportional to



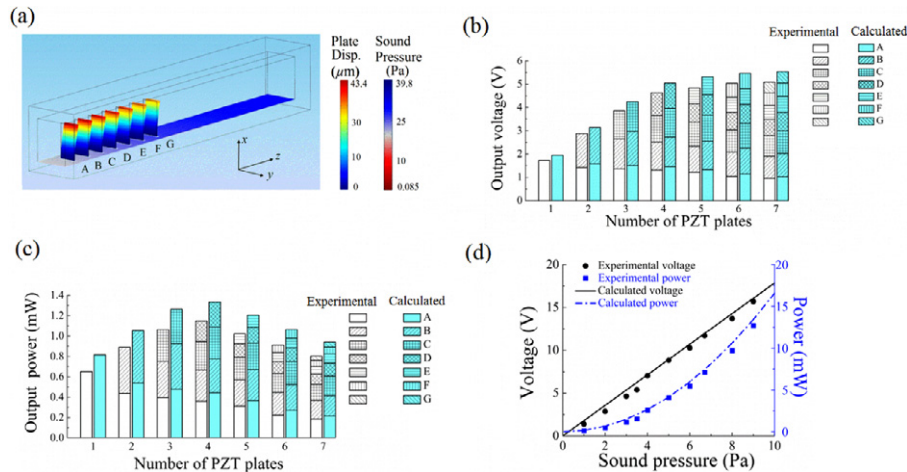


**Figure 7.** (a) An example of the calculated displacements of seven piezoelectric plates placed in the first half of the tube and the sound pressure. Experimental and calculated (b) voltage and (c) power with incident SPL of 100 dB. (d) Total output voltage and power as a function of incident sound pressure using four piezoelectric plates placed at the positions A ( $z = 2.5$  cm) through D ( $z = 10$  cm).

the incident sound pressure, which confirms that the driving force is from the pressure gradient of resonant standing waves. The maximum voltage of 15.689 V has been measured with an incident pressure of 9 Pa (i.e. SPL = 110 dB). The corresponding power is 12.697 mW with areal and volume power densities of  $0.635 \text{ mW cm}^{-2}$  and  $15.115 \mu\text{W cm}^{-3}$ , respectively.

## 6. Conclusion

A novel and practical acoustic energy harvesting mechanism at relatively low audible frequency using the quarter-wavelength straight tube resonator with multiple PZT cantilever plates has been studied experimentally and numerically. The first eigenmode frequency and amplification ratio of the 42 cm-long tube are measured as 199 Hz and 97.2. To convert the first eigenmode acoustic energy in the tube, PZT piezoelectric plates have been placed along the tube axis. With the single PZT plate placed in the tube, the voltage and power become maximum near the open tube inlet where the largest acoustic pressure gradient is available. The voltage and power gradually decrease as the plate is moved to the closed tube end. To increase the total output voltage and power, multiple piezoelectric plates have been placed inside the tube. The number of plates to generate the maximum voltage and power is limited by the interruption of air particle motion. In the experiments, the maximum voltage and power with four PZT plates are 5.089 V and 1.148 mW respectively, with an incident SPL of 100 dB. The voltage increases linearly with the incident sound pressure. At an incident SPL of 110 dB, a voltage of 15.689 V has been measured which corresponds to a power of 12.697 mW with areal and volume power densities of  $0.635 \text{ mW cm}^{-2}$  and  $15.115 \mu\text{W cm}^{-3}$ , respectively.

## References

- [1] Mekhilefa S, Saidurb R and Safari A 2011 A review on solar energy use in industries *Renew. Sustain. Energy Rev.* **15** 1777–90
- [2] Kaldellis J K and Zafirakis D 2011 The wind energy (r)evolution: a short review of a long history *Renew. Sustain. Energy* **36** 1887–901
- [3] Tang X and Zuo L 2012 Vibration energy harvesting from random force and motion excitations *Smart Mater. Struct.* **21** 075025
- [4] Parameshwarana R, Kalaiselvam S, Harikrishnan S and Elayaperumal A 2012 Sustainable thermal energy storage technologies for buildings: a review *Renew. Sustain. Energy Rev.* **16** 2394–433
- [5] Yang R, Qin Y, Li C, Zhu G and Wang Z L 2009 Converting biomechanical energy into electricity by a muscle-movement-driven nanogenerator *Nano Lett.* **9** 1201–5
- [6] Horowitz S B, Sheplak M, Cattafesta L N and Nishida T 2006 A MEMS acoustic energy harvester *J. Micromech. Microeng.* **16** S174–81
- [7] Manglarotty R A 1973 Acoustic-lining concepts and materials for engine ducts *J. Acoust. Soc. Am.* **48** 783–94
- [8] Liu F, Phipps A, Horowitz S, Ngo K, Cattafesta L, Nishida T and Sheplak M 2008 Acoustic energy harvesting using an electromechanical Helmholtz resonator *J. Acoust. Soc. Am.* **123** 1983–90
- [9] Liu F, Horowitz S, Nishida T, Cattafesta L and Sheplak M 2007 A multiple degree of freedom electromechanical Helmholtz resonator *J. Acoust. Soc. Am.* **122** 291–301
- [10] Phipps A, Liu F, Cattafesta L, Sheplak M and Nishida T 2009 Demonstration of a wireless, self-powered, electroacoustic liner system *J. Acoust. Soc. Am.* **125** 873–81
- [11] Kim S H, Ji C H, Galle P, Herrault F, Wu X, Lee J H, Choi C A and Allen M G 2009 An electromagnetic energy scavenger from direct airflow *J. Micromech. Microeng.* **19** 094010
- [12] Wu L Y, Chen L W and Liu C M 2009 Acoustic energy harvesting using resonant cavity of a sonic crystal *Appl. Phys. Lett.* **95** 013506
- [13] Wang W C, Wu L Y, Chen L W and Liu C M 2010 Acoustic energy harvesting by piezoelectric curved beams in the cavity of a sonic crystal *Smart Mater. Struct.* **19** 045016
- [14] Wu L Y, Chen L W and Liu C M 2009 Acoustic pressure in cavity of variously sized two-dimensional sonic crystals with various filling fractions *Phys. Lett. A* **373** 1189–95
- [15] Lallart M, Guyomar D, Richard C and Petit L 2010 Nonlinear optimization of acoustic energy harvesting using piezoelectric devices *J. Acoust. Soc. Am.* **128** 2739–48



- [16] Bork I 1995 Practical tuning of xylophone bars and resonators *Appl. Acoust.* **46** 103–27
- [17] Tang S K 2010 On sound transmission loss across a Helmholtz resonator in a low Mach number flow duct *J. Acoust. Soc. Am.* **127** 3519–25
- [18] Alster M 1972 Improved calculation of resonant frequencies of Helmholtz resonators *J. Sound Vib.* **24** 63–85
- [19] Blackstock D 2000 *Fundamentals of Physical Acoustic* (New York: Wiley)
- [20] Roundy S and Wright P K 2004 A piezoelectric vibration based generator for wireless electronics *Smart Mater. Struct.* **13** 1131–42
- [21] Roundy S, Wright R K and Rabaey J M 2003 *Energy Scavenging for Wireless Sensor Networks with Special Focus on Vibration* (Norwell: Kluwer Academic)
- [22] Koyama D and Nakamura K 2010 Electric power generation using vibration of a polyurea piezoelectric thin film *Appl. Acoust.* **71** 439–45
- [23] Lu F, Lee H P and Lim S P 2004 Modeling and analysis of micro piezoelectric power generators for micro-electromechanical-systems applications *Smart Mater. Struct.* **13** 57–63
- [24] Hibbeler R 2008 *Mechanics of Materials* (New Jersey: Pearson Prentice Hall)